Part III Optical Properties of Materials

Measurement of optical properties : ~ 40 techniques

- Kramers-Kronig Analysis (Dispersion Relations)

- Spectroscopic Ellipsometry

- Differential Reflectometry

13.1.1 Kramers-Kronig Analysis (Dispersion Relations)

A relationship between real and imaginary term of any complex function, which enables one to calculate one component of a complex quantity if the other one is known: phase jump δ''(between the reflected and incident ray) from the reflectivity, R, which was measured at a given frequency, v:

Kramers-Kronig relation

$$\delta'(v_x) = \frac{1}{\pi} \int_0^\infty \frac{d \ln \rho}{dv} \ln \left| \frac{v + v_x}{v - v_x} \right| dv$$

where $\rho = \sqrt{R} = \sqrt{\frac{I_R}{I_0}}$

The optical constants are calculated by applying

$$n = \frac{1 - \rho^2}{1 + \rho^2 + 2\rho \cos \delta'} \qquad k = \frac{2\rho \sin \delta'}{1 + \rho^2 + 2\rho \cos \delta'}$$
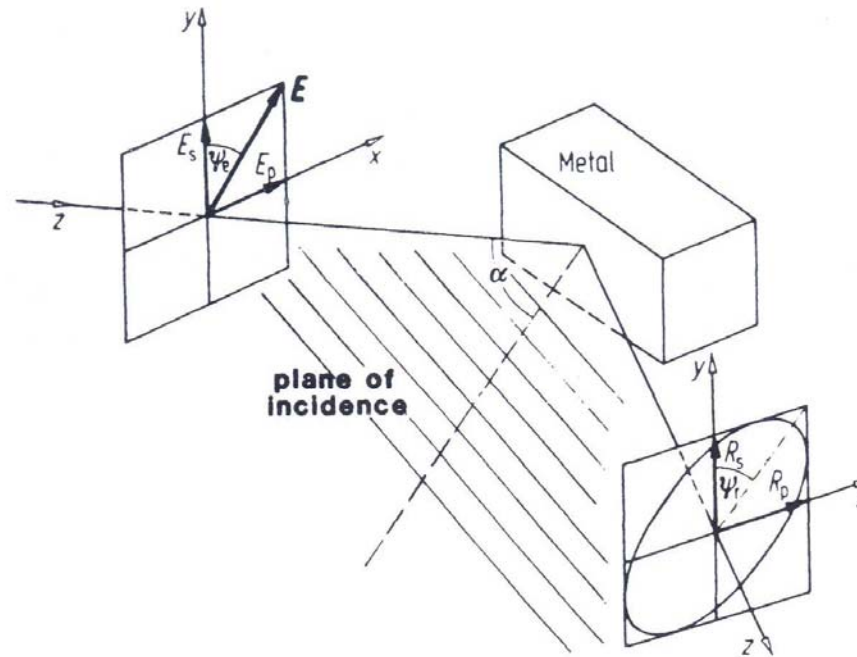
13.1.2 Spectroscopic Ellipsometry

Figure 13.1. Reflection of plane-polarized light on a metal surface. (*Note*: In the figure $\mathscr{E}_{Rp} \equiv R_p$ and $\mathscr{E}_{Rs} \equiv R_s$.)

If a plane-polarized light impinges under an angle α on a metal, the reflected light is generally elliptically polarized. The analysis of this elliptically polarized light yields two parameters, the **azimuth** and the **phase difference**, from which the optical properties are calculated.
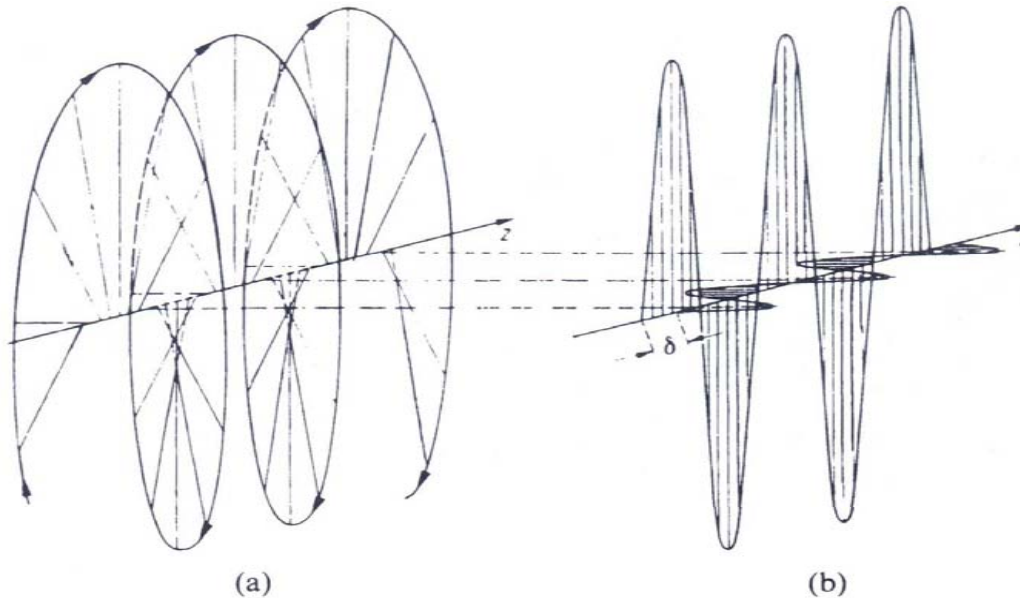
13.1.2 Spectroscopic Ellipsometry

Figure 13.2. (a) Elliptically polarized light and (b) decomposition of elliptically polarized light into two mutually perpendicular plane-polarized waves with phase difference δ. Adapted from R.W. Pohl, *Optik und Atomphysik*. Springer-Verlag, Berlin (1958).

The tip of the light vector moves along a continuous screw, having the direction of propagation as an axis. Elliptically polarized light can be thought of as composed of two mutually perpendicular, plane-polarized waves, having a phase difference δ between them.
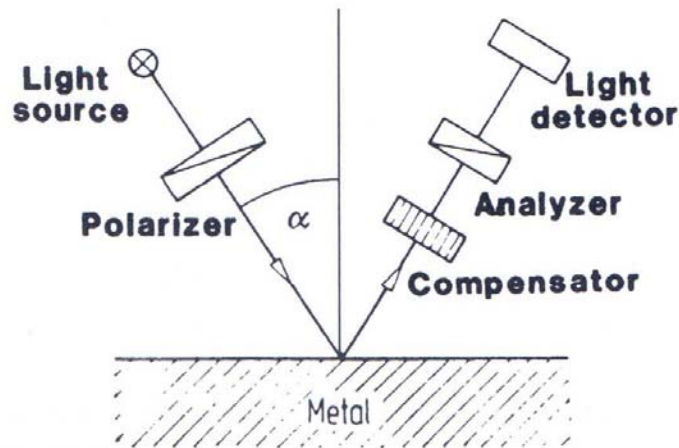
13.1.2 Spectroscopic Ellipsometry

Figure 13.3. Schematic of an **ellipsometer** (polarizer and analyzer are identical devices).

For the actual measurement of ψ_r (the azimuth of reflected light) and δ (the phase difference), one needs two polarizers consisting of a birefringent material, which allows only plane-polarized light to pass, and a compensator also consisting of birefringent material, which allows one to measure the phase difference δ.
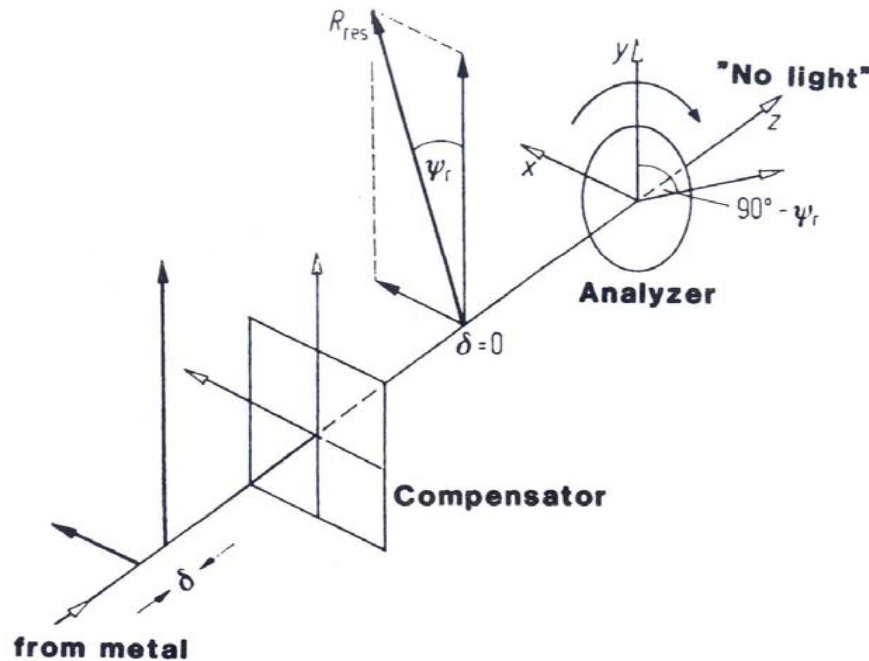
13.1.2 Spectroscopic Ellipsometry

Figure 13.4. Vector diagram of light reflected from a metal surface. The vectors having solid arrowheads give the vibrational direction and magnitude of the light.

The light reflected from a metal is represented by two light vectors pointing in the *x*- and *y*- directions. Are measured by simultaneously altering the thickness of the compensator and tuning the analyzer until no light leaves the analyzer.

13.1.2 Spectroscopic Ellipsometry

The optical constants are calculated using

$$n^2 = \frac{1}{2}\left[\sqrt{(a^2 - b^2 + \sin^2\alpha)^2 4a^2b^2} + a^2 - b^2 + \sin^2\alpha\right]$$

$$k^2 = \frac{1}{2}\left[\sqrt{(a^2 - b^2 + \sin^2\alpha)^2 4a^2b^2} + a^2 - b^2 + \sin^2\alpha\right]$$

with $\quad a = \dfrac{\sin\alpha\tan\alpha\cos 2\psi_r}{1 - \cos\delta\sin 2\psi_r} \quad b = -a\sin\delta\tan 2\psi_r$

Alternatively, one obtains, for the polarization ε_1 and absorption ε_2

$$\varepsilon_1 = n^2 - k^2 = \sin^2\alpha\left[1 + \frac{\tan^2\alpha(\cos^2 2\psi_r - \sin^2 2\psi_r \sin^2\delta)}{(1 - \sin 2\psi_r \cos\delta)^2}\right]$$

$$\varepsilon_2 = 2nk = -\frac{\sin 4\psi_r \sin\delta\tan^2\alpha\sin^2\alpha}{(1 - \sin 2\psi_r \cos\delta)^2}$$

13.1.3 Differential Reflectometry

A differential reflectogram allows the direct measurement of the energies that electrons absorb from photons as they are raised into higher allowed energy states.

The differential reflectometer measures the normalized difference between the reflectivities of two similar specimens which are mounted side by side. (Fig. 13.5)

It belongs to a family of techniques, called modulation spectroscopy, in which the derivative of the unperturbed reflectivity (or ε_2) with respect to an external parameter is measured. (Fig. 13.6)

13.2 .1 Reflection Spectra

The spectral dependence of the optical properties of metals

- Light interacts with a certain number of free electrons and a certain number of classical harmonic oscillators, or equivalently, by intraband and interband transition
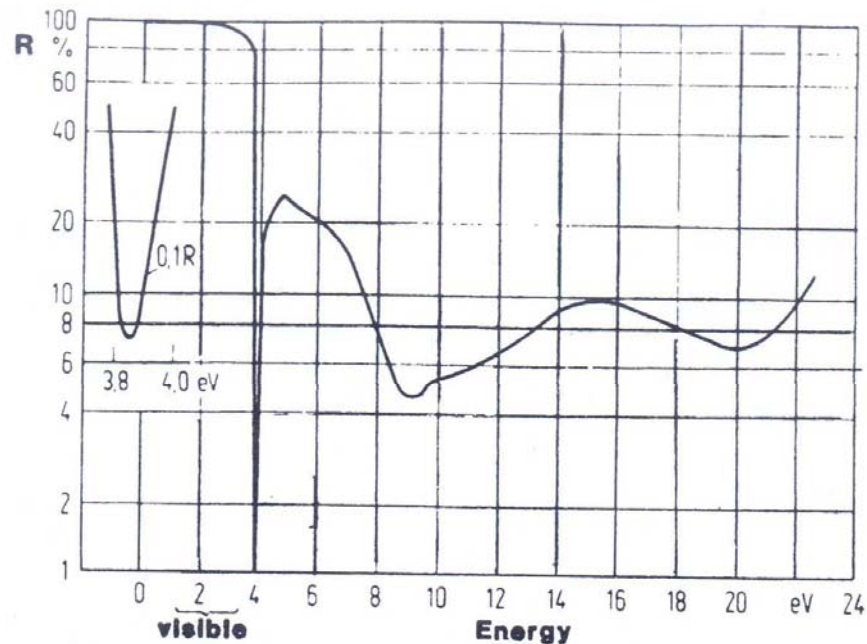
- Silver

Figure 13.7. Reflectivity spectrum for silver. Adapted from H. Ehrenreich et al., *IEEE Spectrum* **2**, 162 (1965). © 1965 IEEE.

13.2 .1 Reflection Spectra

Figure 13.8. Spectral dependence of ε_1 and ε_2 for silver. ε_1 and ε_2 were obtained from Fig. 13.7 by a Kramers–Kronig analysis. Adapted from H. Ehrenreich et al., *IEEE Spectrum* **2**, 162 (1965). © 1965 IEEE.
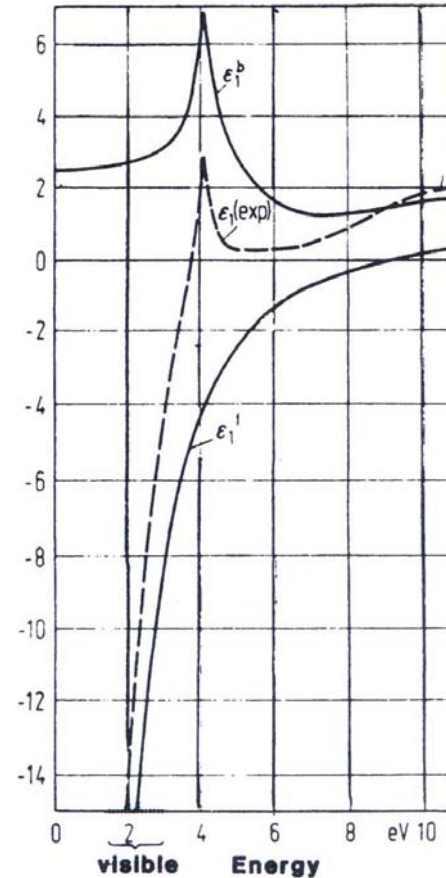
Figure 13.9. Separation of ε_1 for silver into ε_1^f (free electrons) and ε_1^b (bound electrons). Adapted from H. Ehrenreich et al., *IEEE Spectrum* **2**, 162 (1965). © 1965 IEEE.

For $E < 3.8$ eV: the spectral dependence of ε_1 and ε_2 have the characteristic curve shapes for free electrons

13.2 .1 Reflection Spectra

- Copper

Figure 13.11. Spectral dependence of ε_1 and ε_2 for copper. ε_1 and ε_2 were obtained from Fig. 13.10 by a Kramers–Kronig analysis. Adapted from H. Ehrenreich et al., *IEEE Spectrum* **2**, 162 (1965). © 1965 IEEE.
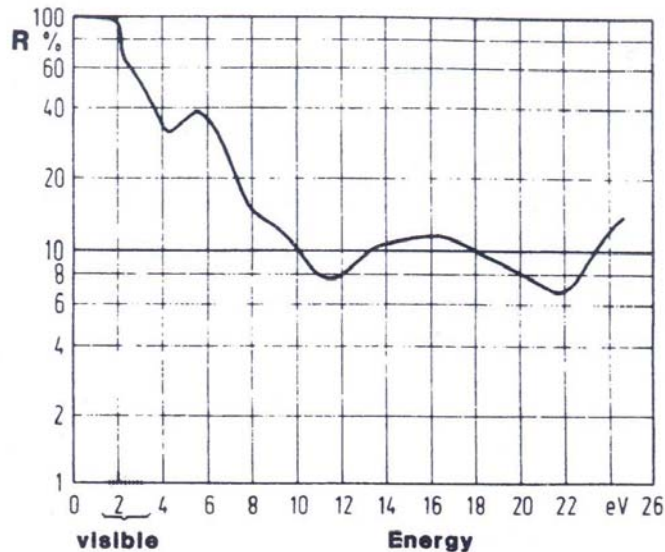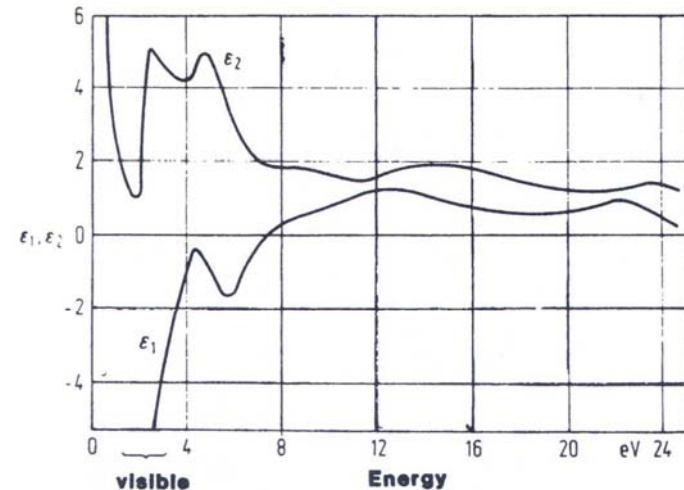

Figure 13.10. Reflectivity spectrum for copper. Adapted from H. Ehrenreich et al., *IEEE Spectrum* **2**, 162 (1965). © 1965 IEEE.

Copper possesses an absorption band in the visible spectrum, which is responsible for the characteristic color of copper.

13.2 .1 Reflection Spectra

- Aluminum

Figure 13.13. Spectral dependence of ε_1 and ε_2 for aluminum. Adapted from H. Ehrenreich et al., *IEEE Spectrum* **2**, 162 (1965). © 1965 IEEE.

"Free electron-like behavior"

Figure 13.12. Reflection spectrum for aluminum. Adapted from H. Ehrenreich et al., *IEEE Spectrum* **2**, 162 (1965). © 1965 IEEE.
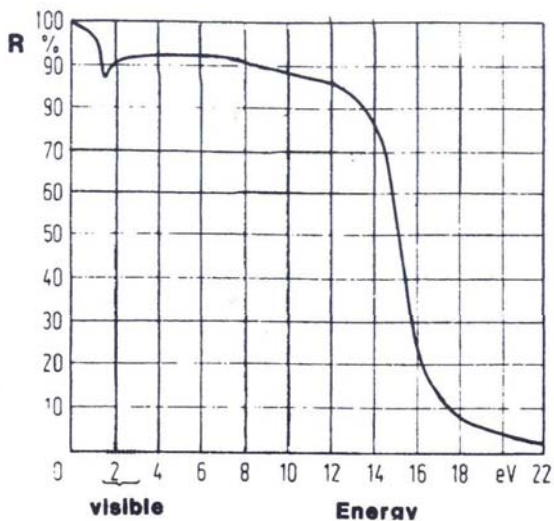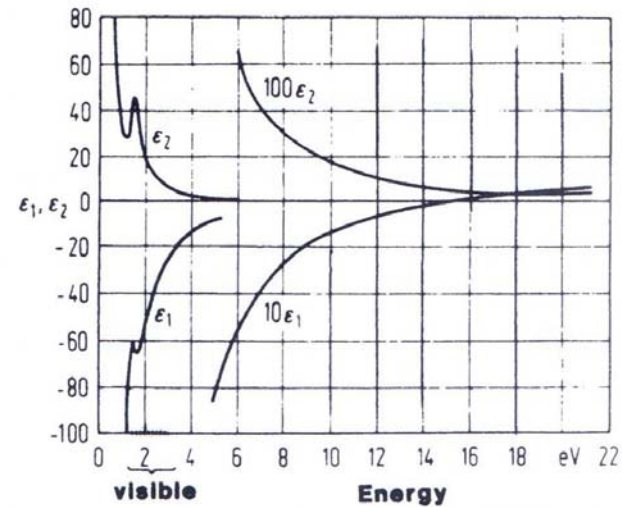
13.2 Optical Spectra of Pure Metals

* 13.2 .2 Plasma Oscillations

We postulate that the free electrons of a metal interact electrostatically, thus forming an electron "**plasma**" that can be excited by light of proper photon energy to collectively perform fluidlike oscillations.

At the **plasma frequency**, $\hat{\varepsilon}$ (ε_1 as well as ε_2) must be zero.

$$\hat{\varepsilon} = \varepsilon_1 - i\varepsilon_2 = 0$$

The frequency dependence of the imaginary part of the reciprocal dielectric constant peaks at the plasma frequency

$$\frac{1}{\hat{\varepsilon}} = \frac{1}{\varepsilon_1 - i\varepsilon_2} = \frac{\varepsilon_1 + i\varepsilon_2}{\varepsilon_1^2 + \varepsilon_2^2} = \frac{\varepsilon_1}{\varepsilon_1^2 - \varepsilon_2^2} + i\frac{\varepsilon_2}{\varepsilon_1^2 + \varepsilon_2^2}$$

The imaginary part of the reciprocal dielectric constant

$$\mathrm{Im}\frac{1}{\hat{\varepsilon}} = \frac{\varepsilon_2}{\varepsilon_1^2 + \varepsilon_2^2} \qquad \text{"energy loss function"}$$

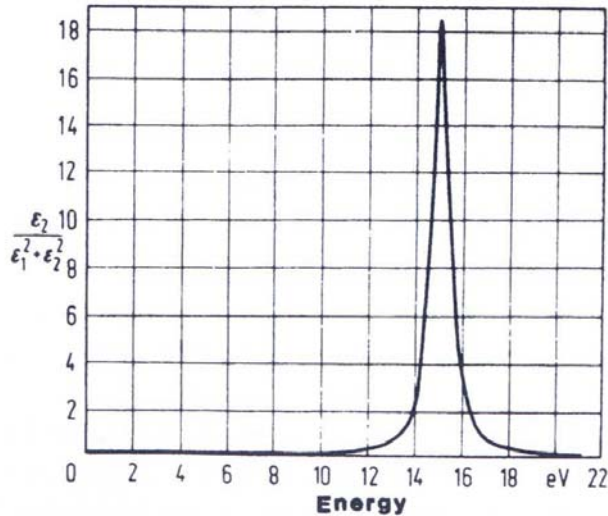## *13.2 .2 Plasma Oscillations

Figure 13.15. Energy loss function for silver. Adapted from H. Ehrenreich et al., *IEEE Spectrum* **2**, 162 (1965). © 1965 IEEE.

Figure 13.14. Energy loss function for aluminum. Adapted from H. Ehrenreich et al., *IEEE Spectrum* **2**, 162 (1965). © 1965 IEEE.

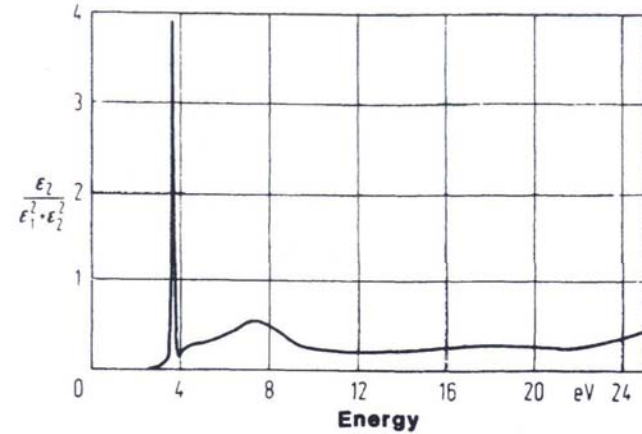N.F. **Mott's suggestion** "when a small amount of metal A is added to a metal B, the Fermi energy would simply assume an average value, while leaving the electron bands of the solvent intact", called "rigid-band model". -> needed some modification.

- Cu-Zn

Fig 13.16 : a series of differential reflectograms from which the energies for interband transitions, E_T can be taken
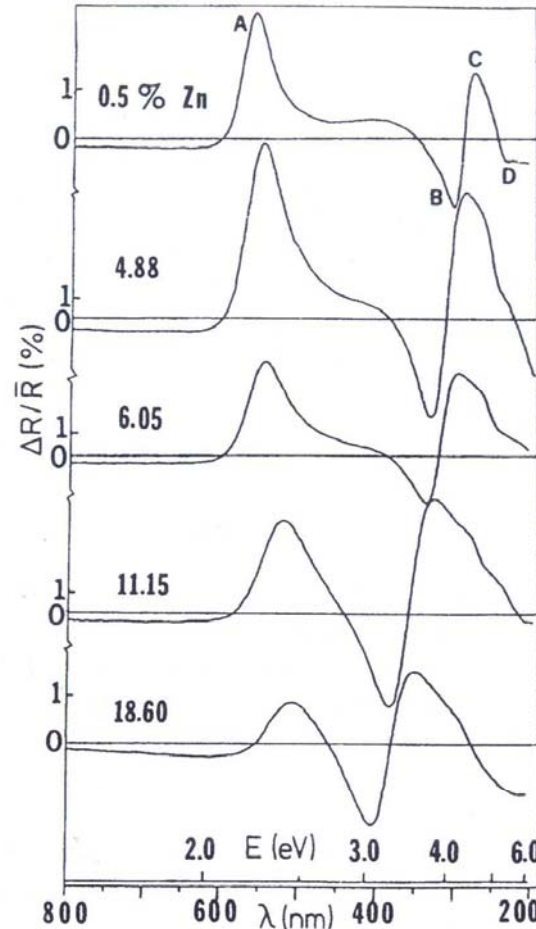

Figure 13.16. Experimental differential reflectograms for various copper–zinc alloys. The parameter on the curves is the average zinc concentration of the two alloys in at.%. The curve marked 0.5%, e.g., resulted by scanning the light beam between pure copper and a Cu–1% Zn alloy. Peaks A and D are designated as ε_2-type structures (Fig. 11.10) whereas features B and C belong to an ε_1-type structure (Fig. 11.9). From R.J. Nastasi-Andrews and R.E. Hummel, *Phys. Rev. B* **16**, 4314 (1977).

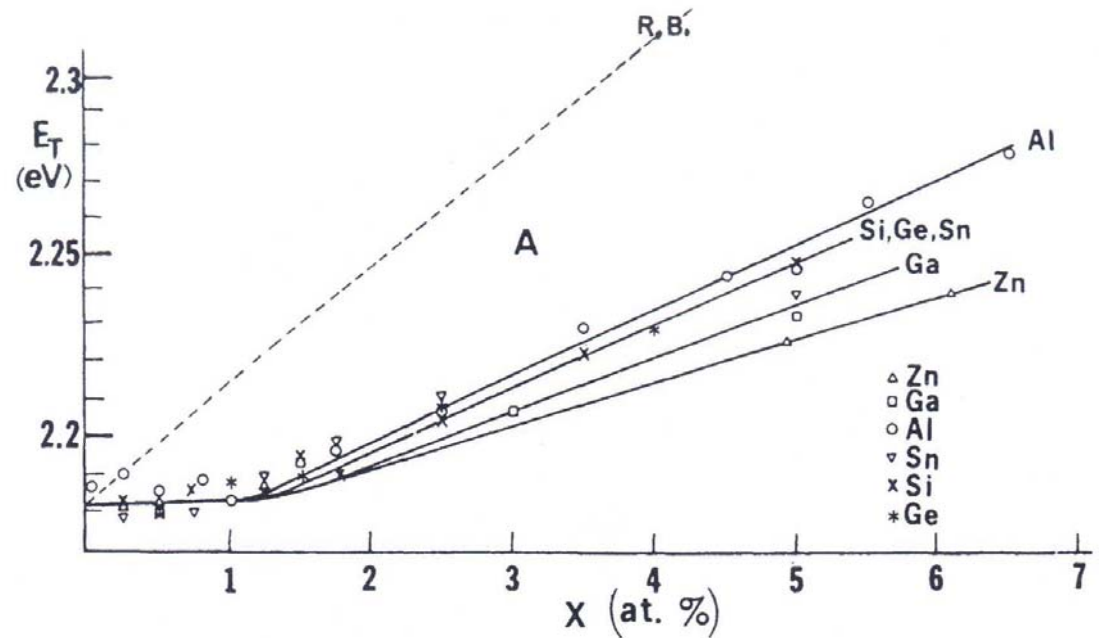A linear increase in E_T with increasing X is observed

Figure 13.17. Threshold energies, E_T, for interband transitions for various copper-based alloys as a function of solute content. The E_T values are taken from differential reflectograms similar to those shown in Fig. 13.16. The rigid band line (R.B.) for Cu–Zn is added for comparison. From R.J. Nastasi-Andrews and R.E. Hummel, *Phys. Rev. B* **16**, 4314 (1977).
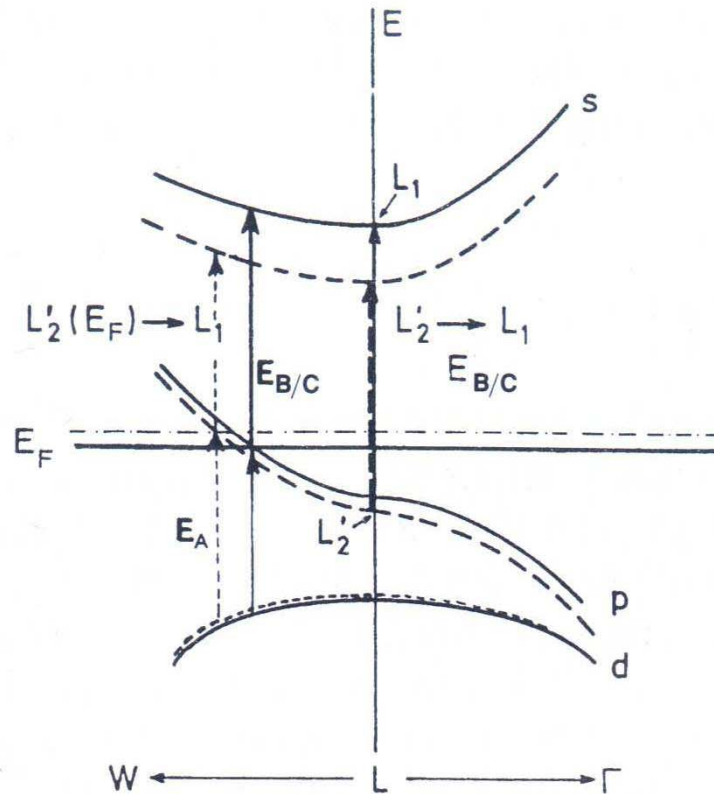
Figure 13.18. Schematic band structure near L for copper (solid lines) and an assumed dilute copper-based alloy (dashed lines). Compare with Figs. 12.3 and 5.22.
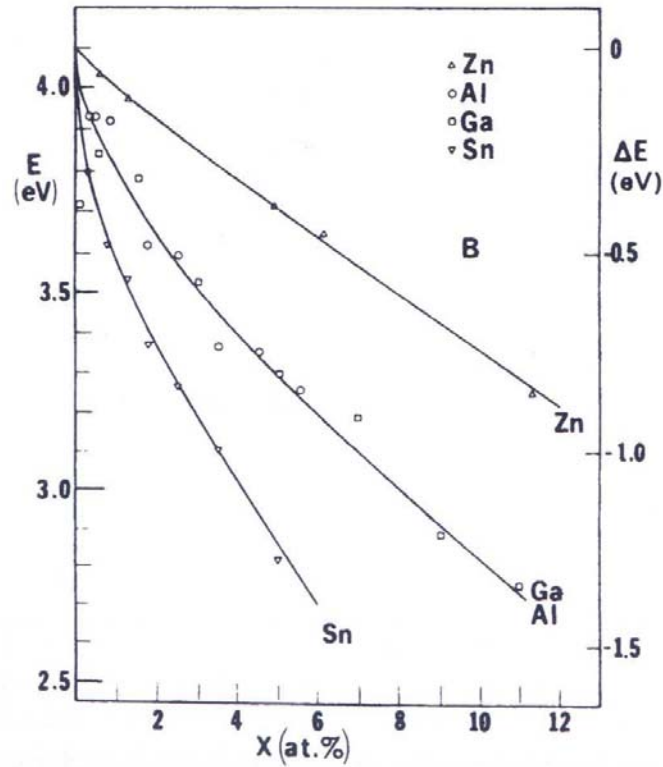
Figure 13.19. Energy of peak B for various dilute copper-based alloys. From R.J. Nastasi-Andrews, and R.E. Hummel, *Phys. Rev. B* **16**, 4314 (1977).

*13.4 Ordering

(In Sec. 7.5.3, resistivity decreases when solute atoms of an alloy are periodically arranged) The ordering has an effect on the electronic structure and hence on the optical properties of alloys

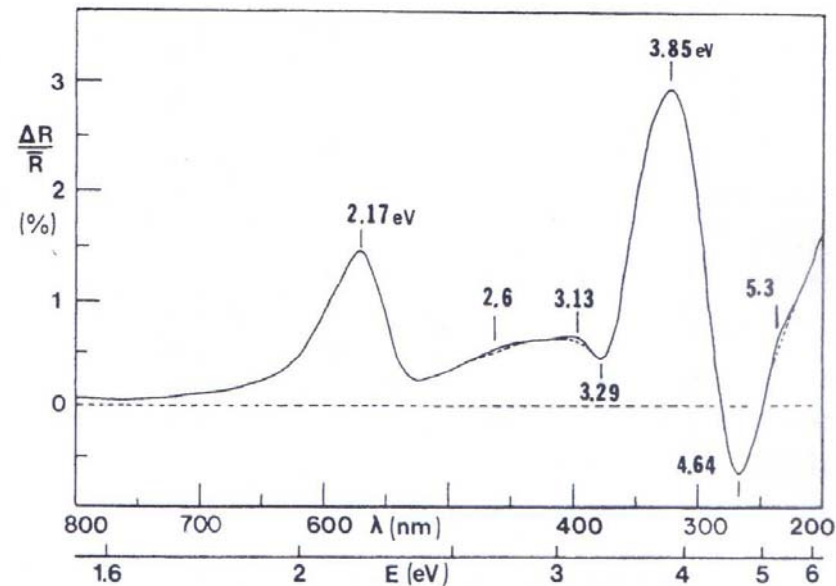Fig 13.20 : an optical spectrum for the intermetallic phase Cu_3Au

Figure 13.20. Differential reflectogram of (long-range) ordered versus disordered Cu_3Au. From R.E. Hummel, *Phys. Stat. Sol.* (a) **76**, 11 (1983).

Short-range ordering shows comparatively smaller effects than long-range ordering
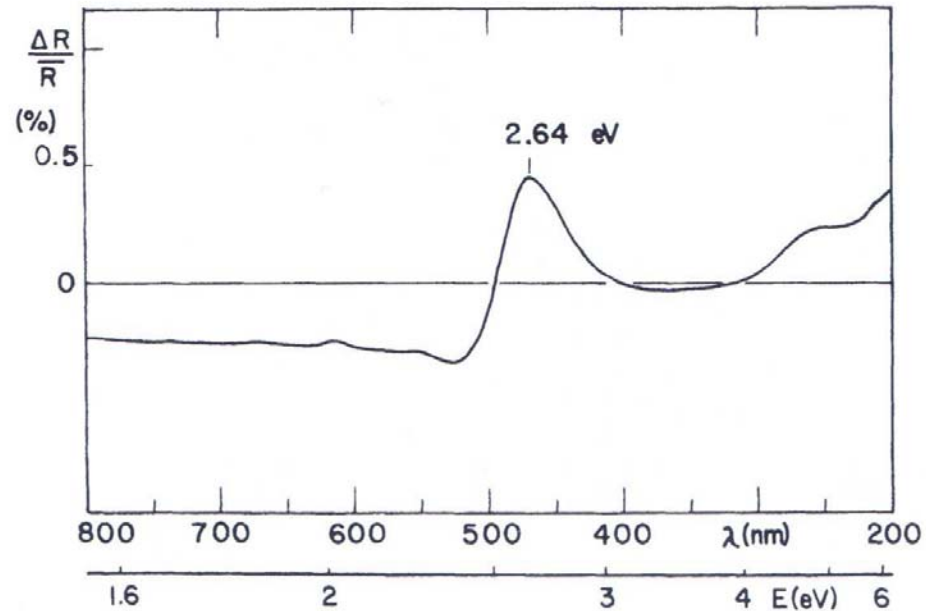

Figure 13.22. Differential reflectogram of (short-range) ordered versus disordered Cu–17 at.% Al. From J.B. Andrews, R.J. Andrews, and R.E. Hummel, *Phys. Rev. B* **22**, 1837 (1980).

"Electrochemical corrosion of copper in an aqueous solution"

- Fig 13.23 : a series of differential reflectograms demonstrating the evolution of Cu_2O on a copper substrate
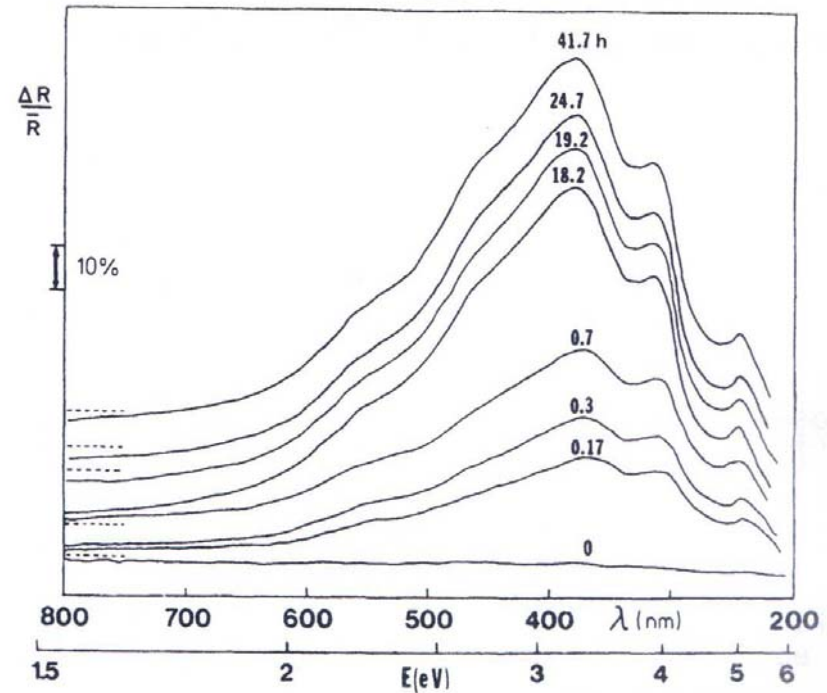

Figure 13.23. Differential reflectograms depicting the *in situ* evolution of Cu_2O on a copper substrate in a buffered electrolyte of pH 9. One sample half was held potentiostatically at −200 mV (SCE) for various times, the other at the protective potential (−500 mV (SCE)). From R.E. Hummel, *Phys. Stat. Sol.* (a) **76**, 11 (1983).

- The optical behavior of an intrinsic semiconductor is similar to that of an insulator : it is transparent in the low energy (far IR) region

- Once the energy of photons are excited from the top of the valence band to the bottom of the conduction band. The semiconductor becomes opaque like a metal (Fig 13.24)
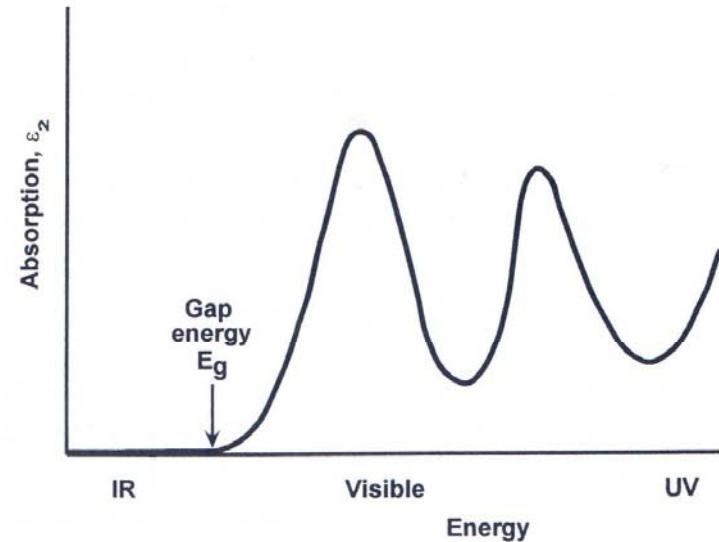

Figure 13.24. Schematic representation of the absorption spectrum of an intrinsic, direct–band gap semiconductor. The material is transparent below the gap energy and opaque above E_g.

- The onset for *inter*band transitions is thus determined by the gap energy, which characteristically values between 0.2eV and 3.5eV

Fig 13.25

- Three distinct absorption peaks :

$L_3 \rightarrow L_1$ (3.4 eV),

Σ (4.2 eV),

$L'_3 \rightarrow$ (5.6 eV)

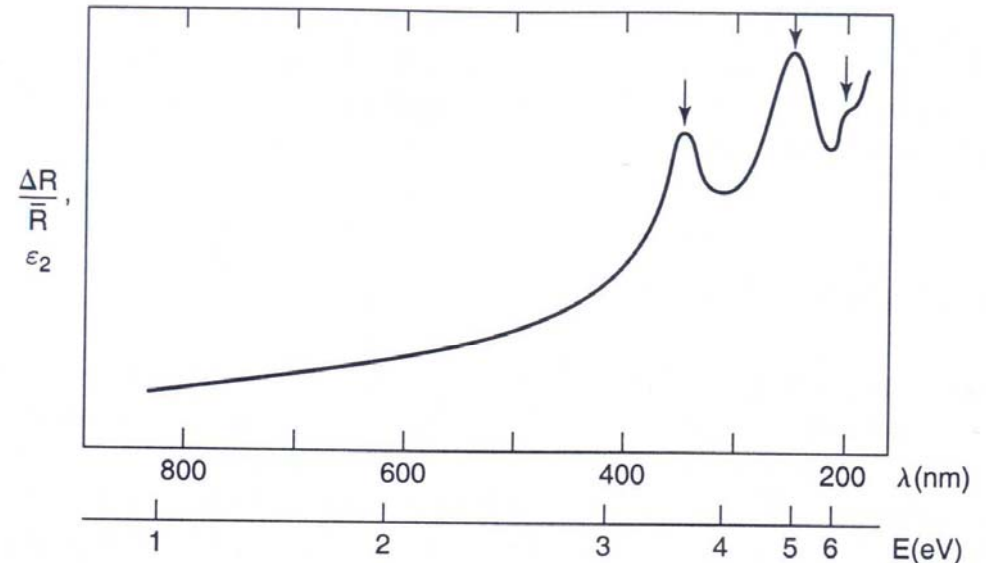- These peaks are all caused by direct interband transitions in specific area of *k*-space

Figure 13.25. Differential reflectogram of silicon (after R.E. Hummel and W. Xi). $\Delta R/\bar{R}$ is essentially the absorption, ε_2, as explained in Section 13.1.3

- Direct and indirect transition (Fig 13.26) : indirect transitions between the top of the valence band and the bottom of the conduction band may be possible to a limited degree provided the necessary momentum (wave vector *k*) is furnished by a photon
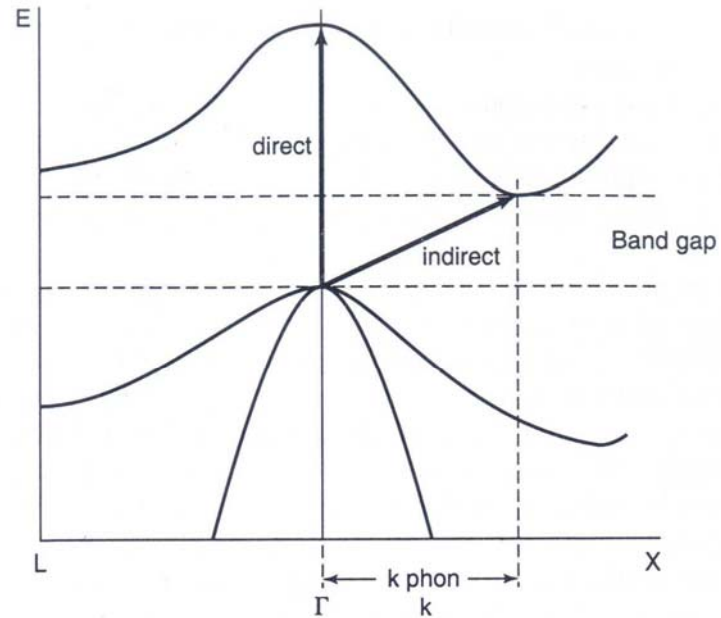

Figure 13.26. Schematic representation of direct versus indirect interband absorptions in Si. In the case of an indirect transition, a phonon needs to be additionally absorbed. Compare to Fig. 5.23 and 12.2.

13.6 Semiconductors

Absorption spectra for semiconductors show a structure for photon energies slightly below the gap energy (Fig 13.27a)

- Frenkel explained this behavior by postulating that a photon may excite an electron so that it remains in the vicinity of its nucleus,

Figure 13.27. (a) Spectral dependence of the absorbance, α, (10.21a) for gallium arsenide at 21 K. Adapted from M.D. Sturge, *Phys. Rev.* **127**, 768 (1962). (b) Schematic representation of exciton energy levels and an exciton in a semiconductor (or insulator).

thus forming an electron-hole pair, called an **exciton**

- One depicts the excitons by introducing "exciton levels" into the forbidden band (Fig 13.27b)

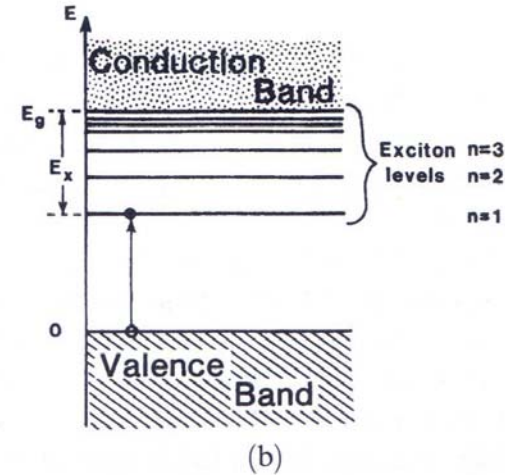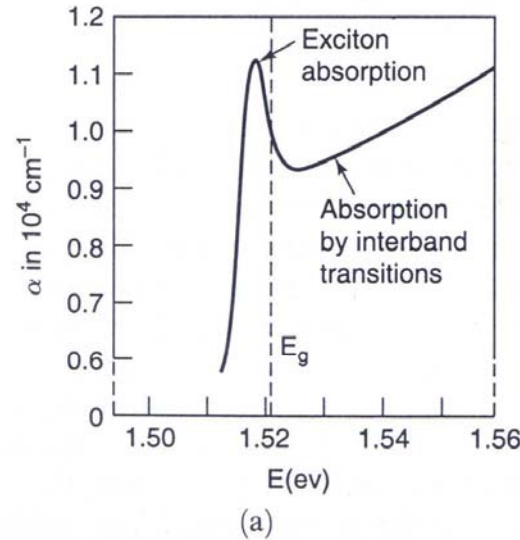binding energy, $\quad E_x = -\dfrac{m^* e^4}{(4\pi\varepsilon_0)^2 \, 2n^2 \hbar^2 \varepsilon^2}$

- Insulators are characterized by completely filled valence bands and empty "conduction" bands : no intraband transition, i.e., no classical IR absorption

- Light-induced vibration of lattice atoms : **excitation of phonons by photons**
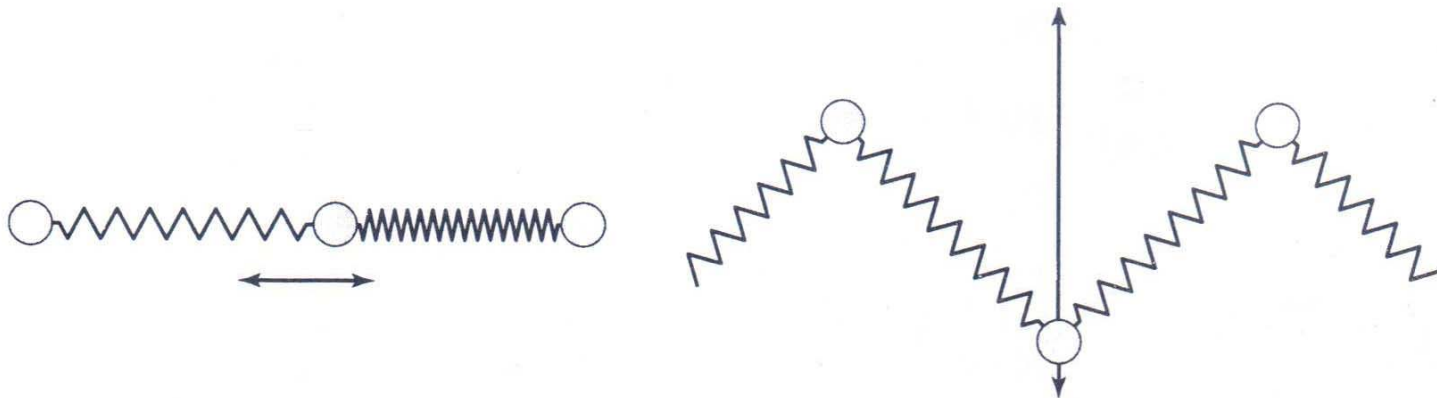

Figure 13.28. One-dimensional representations of possible vibration modes of atoms that have been excited by IR electromagnetic radiation (heat).

- Monoatomic crystal (one kind of atom)

oscillations of atoms under the influence of light whose excitation force is $eE_0 \exp(i\omega t)$

$$m \frac{d^2 x}{dt^2} + \gamma' \frac{dx}{dt} + kx = eE_0 \exp(i\omega t)$$

- Diatomic solids : two differential equations of the above type need to be written; 2N coupled differential equations, where N is the number of unit cells in the lattice. The resonance frequency for diatomic crystals is

$$\omega_0 = 2k \left(\frac{1}{m_1} + \frac{1}{m_2} \right)$$

Fig 13.29 : the spectral reflectivity of NaCl in the IR. Sodium chloride is transmissive between 0.04 eV and 7 eV
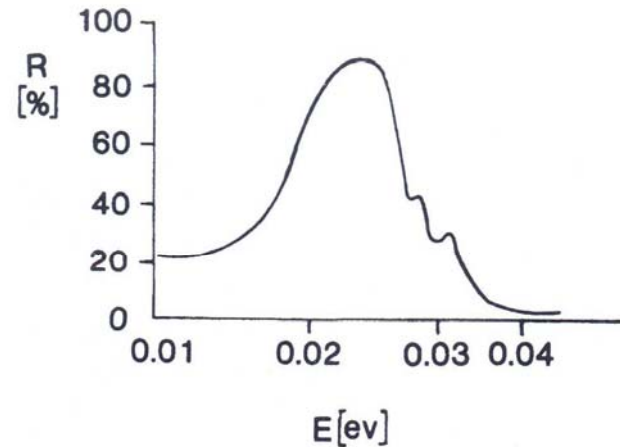

Figure 13.29. Spectral reflectivity of NaCl at room temperature in the far IR region.

Fig 13.30 : The absorption spectrum for the commercially important **borosilicate/phosphosilicate glass**, used for **optical fibers**
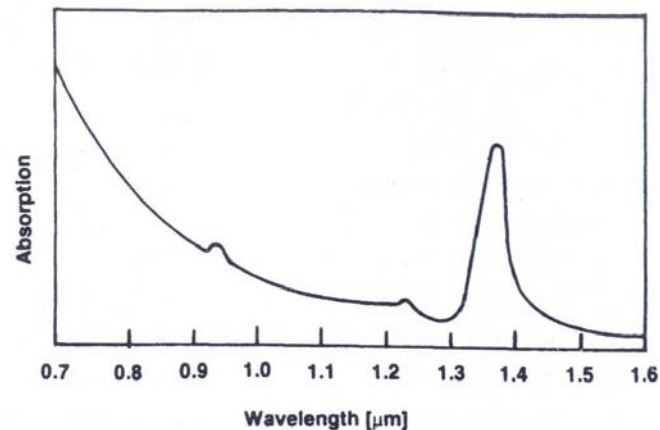

Figure 13.30. Absorption spectrum of highly purified glass for fiber-optic applications which features a phosphosilicate core surrounded by a borosilicate cladding.

13.8 Emission of Light

13.8.1 Spontaneous Emission

luminescence : the emission of light due to reversion of electron from a higher energy state

 - **fluorescence** : the electron transition occurs within nanoseconds of faster

 - **phosphorescence**: the emission takes place after microseconds or milliseconds (slower process)

- **afterglow** : even slower (seconds), occurs when excited electrons have been temporarily trapped in impurity states from which they eventually return after some time into the valence band

13.8 Emission of Light

13.8.1 Spontaneous Emission

- **Photoluminescence** is observed when photons impinge on a material which in turn re-emits light of a lower energy.

- **Electroluminescing** materials emit light as a consequence of an applied voltage or electric field.

- **Cathodoluminescence** is term which is used to describe light emission from a substance that has been showered by electrons of higher energy

- **Thermoluminescence** Spontaneous light emission occurs also in common devices such as candles or incandescent light bulbs. In both of these cases, the electrons have been excited into higher energy states by heat energy.

13.8.2 Stimulated Emission (Lasers)

LASER: *light amplification by stimulated emission of radiation*

- applications: telecommunications (optical fiber networks), data storage (compact discs), laser printers, and grocery scanners

- population inversion of electrons (Fig 13.31a)

- a photon energy E_{21} = hν_{21} : **momochromatic**

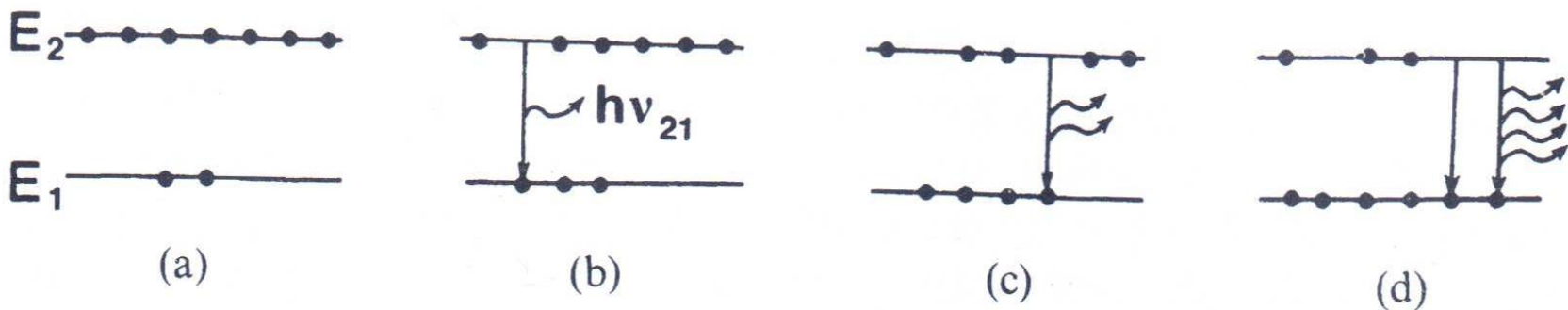- strong **collimation**, i.e., the parallel emergence of light

Figure 13.31. Schematic representation of stimulated emission between two energy levels, E_2 and E_1. The dots symbolize electrons.

13.8.2 Stimulated Emission (Lasers)

- The lasing material is embodied in a long narrow cavity; the two faces at opposite ends of this cavity must be absolutely parallel to each other

- One of the faces is silvered and acts as a perfect mirror, whereas the other face is partially silvered and thus transmits some of the light (Fig. 13.32)

-The laser light is reflected back and forth by these mirror, thus increasing the number of photons during each pass

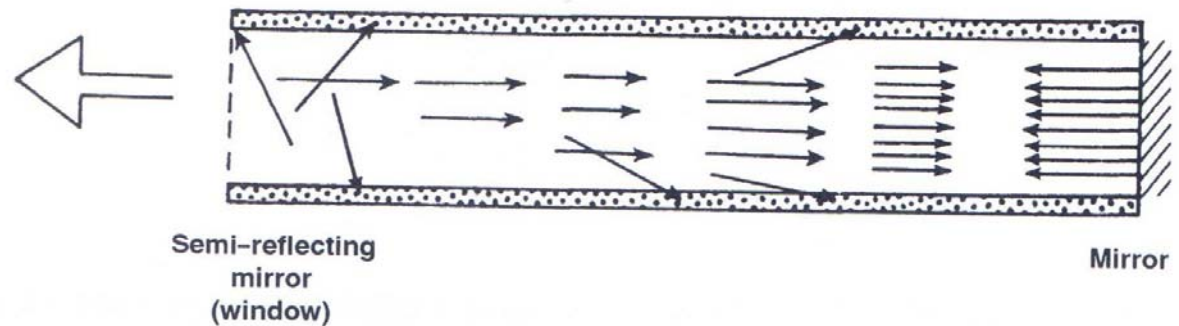Semi–reflecting
mirror
(window)

Mirror

Figure 13.32. Schematic representation of a laser cavity and the buildup of laser oscillations. The stimulated emission eventually dominates over the spontaneous emission. The light leaves the cavity at the left side.
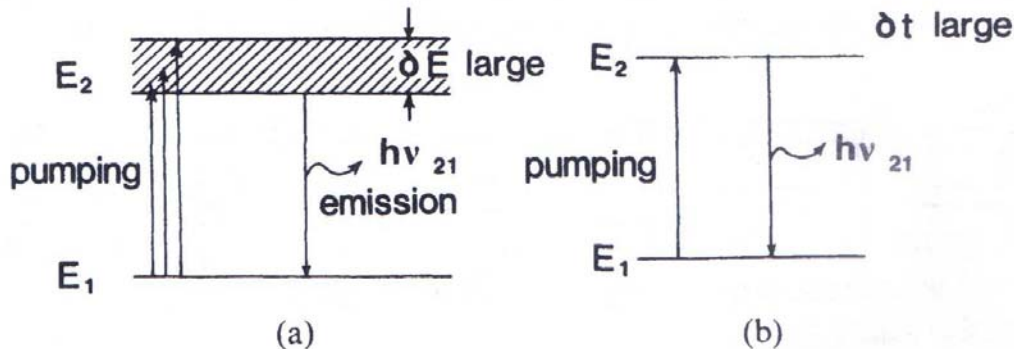
13.8.2 Stimulated Emission (Lasers)

Figure 13.33. Examples of possible energy states in a two-level configuration. (a) δE large, i.e., large pumping efficiency but little or no population inversion. (b) Potentially large population inversion (δt large) but small pumping efficiency. (*Note:* Two-level lasers do not produce a population inversion, because absorption and emission compensate each other.)

Optical pumping : electrons are pumped from E_1 to E_2 ; the absorption of light stemming from polychromatic light source → population inversion

Heisenberg's uncertainty principle : $\delta E \cdot \delta t \propto h$

- The time span, δt, for which an electron remains at the higher energy level, E_2, is large when the bandwidth, δE of E_2 is narrow

13.8.2 Stimulated Emission (Lasers)

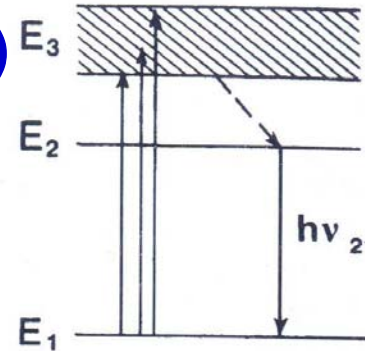**Three-level laser** : the pump band E_3 is broad, which enables a good pumping efficiency

Figure 13.34. Three-level laser. The nonradiative, phonon-assisted decay is marked by a dashed line. Lasing occurs between levels E_2 and E_1. High pumping efficiency to E_3. High population inversion at E_2.
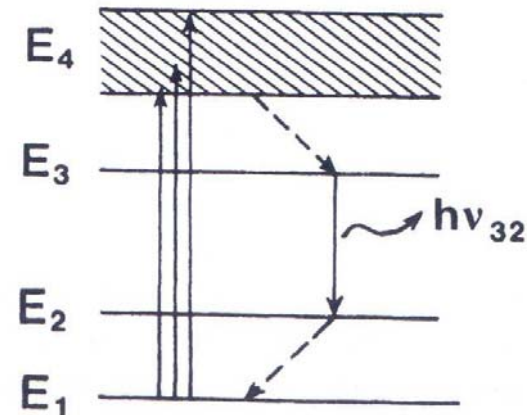
Four-level laser : the energy level E_2 is emptied rapidly by electron transitions into a lower level, E_1

Figure 13.35. Four-level laser.
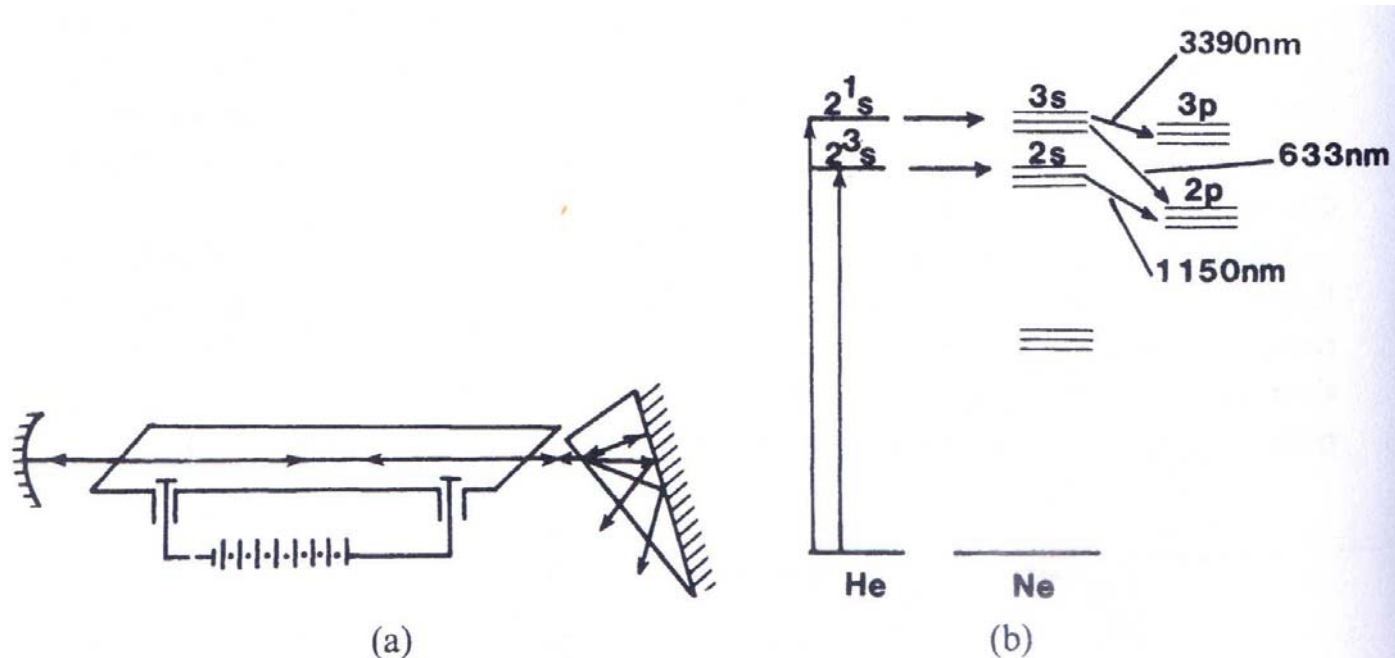
13.8.3 Helium-Neon Laser

Figure 13.36. Helium–neon laser. (a) Schematic diagram of the laser cavity with Littrow prism to obtain preferred oscillation at one wavelength. (The end windows are inclined at the Brewster angle for which plane-polarized light suffers no reflection losses.) (b) Energy level diagram for helium and neon. The decay time for the p-states is $\sim$10 ns; that of the s-states 100 ns. The letters on the energy levels represent the angular momentum quantum number; the number in front of the letters gives the value for the principal quantum number; and the superscripts represent the multiplicity (singlet, doublet, etc.), see Appendix 3.

13.8.4 Carbon Dioxide Laser

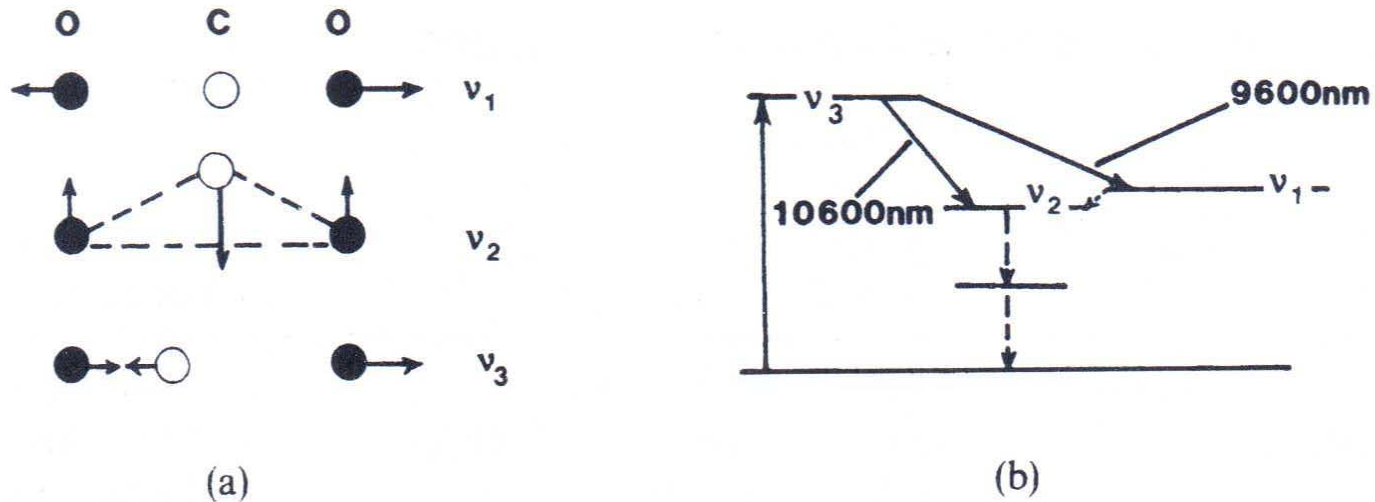Figure 13.37. CO_2 laser. (a) Fundamental modes of vibration for a CO_2 molecule; v_1: symmetric stretching mode; v_2: bending mode; v_3: asymmetric stretching mode. (b) Energy level diagram for various vibrational modes.
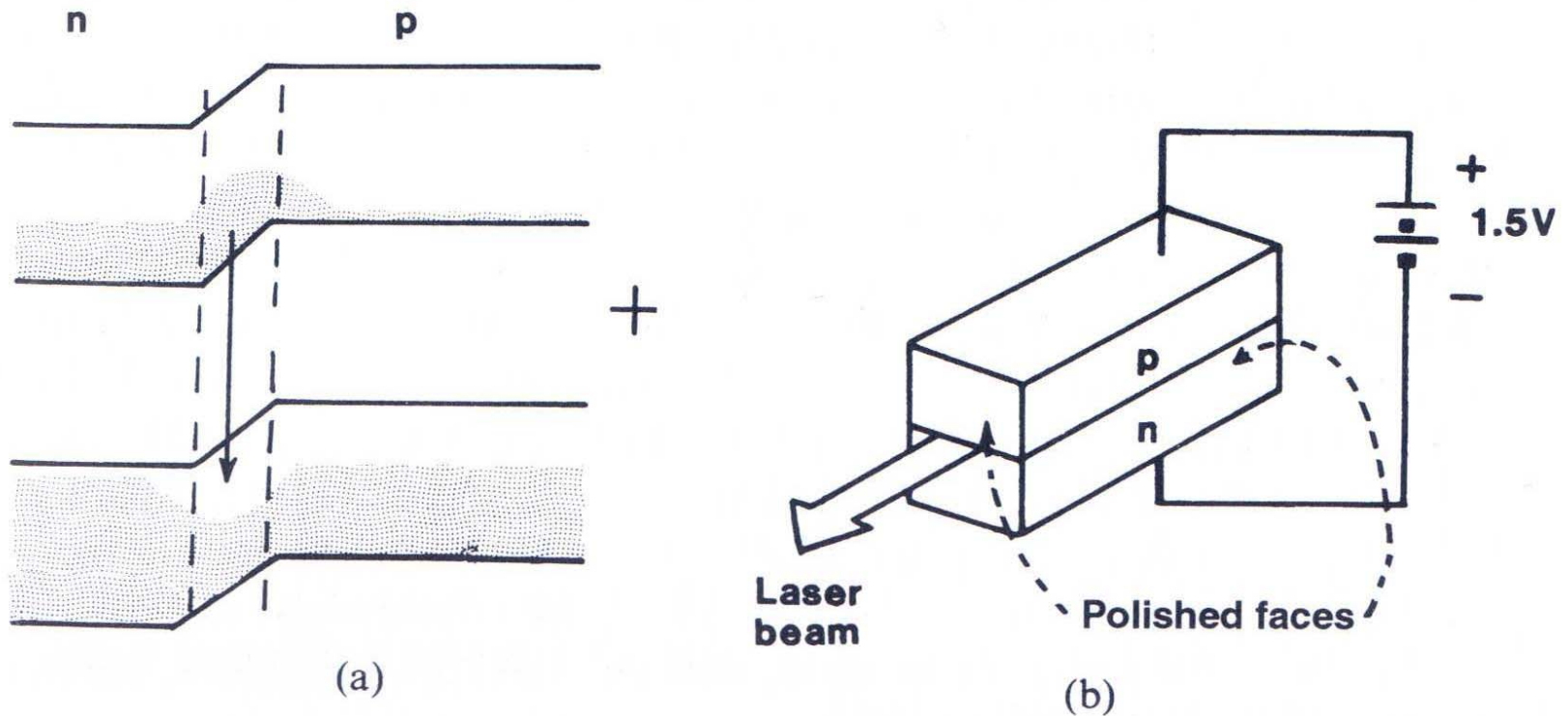
13.8.5 Semiconductor Laser

Figure 13.38. (a) Energy band diagram of a heavily doped, forward-biased semi-conductor. (b) Schematic setup of a semiconductor laser.

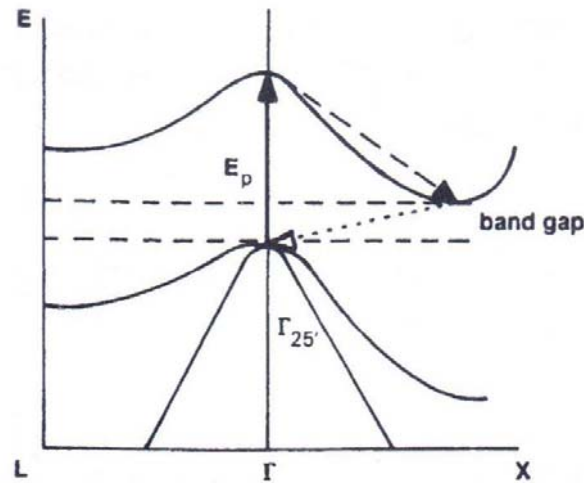## 13.8.6 Direct-Versus Indirect-Band Gap Semiconductor Laser

Figure 13.39. Direct interband transition pumping (E_p) and phonon-involved reversion of a *hot* electron by indirect transitions for an indirect–band gap semiconductor such as silicon. (Compare with Figs. 5.23 and 12.2.)

Indirect-band gap semiconductors (phonon-assisted process involved) seem to be not suited for lasers.

13.8.7 wavelength of Emitted Light

- The band gap, i.e., the wavelength at which a laser emits light, can be adjusted to a certain degree by utilizing ternary or quaternary compound semiconductors
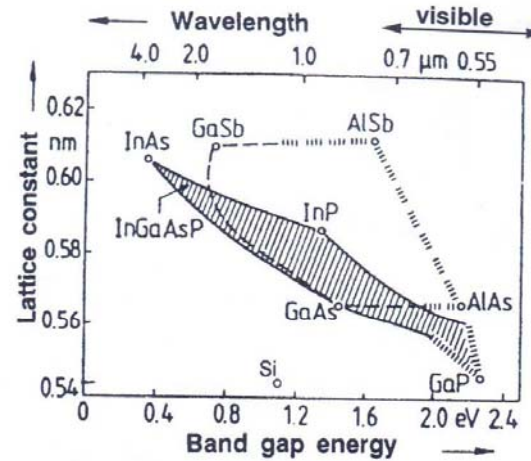
Figure 13.40. Lattice constants, energy gaps, and emission wavelengths of some ternary and quaternary compound semiconductors at 300 K. The lines between the binary compounds denote ternaries. The cross-hatched lines indicate indirect interband transitions. Pure silicon is also added for comparison.

- The emission wavelength depends on the temperature of operation, because the band gap decrease with increasing temperature according to the empirical equation

$$E_{gT} = E_{g0} - \frac{\xi T^2}{T + \theta_D}$$

13.8 Emission of Light

13.8.12 Quantum Well Lasers

- The carriers are confined to a potential well having infinitely high walls.

- The light emission in a quantum well laser occurs as a result of electron transitions from these conduction band levels into valence levels.
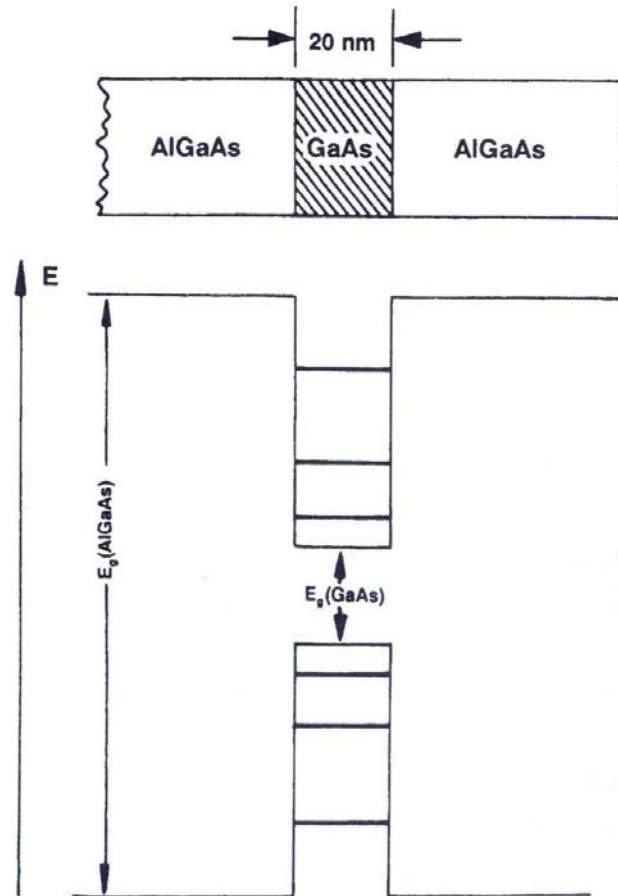

Figure 13.45. Band structure of a single quantum dot structure. See in this context Section 8.7.10 and Fig. 8.33(b).

13.8 Emission of Light

13.8.13 Light-Emitting Diodes (LEDs)

-The LED consists, like semiconductor laser, of a forward biased *p-n* junction

- The light emission occurs in the visible spectrum

- III-V compound semiconductor, such as $Ga_xAs_{1-x}P$, GaP, $Ga_xAl_{1-x}As$ (for red and yellow-green), nitride-based compound semiconductors (for green and blue colors)

- **Chromaticity diagram** : It is based on the peculiarities of the three types of cones in the human eyes which are sensitive for either blue, green, or red radiation
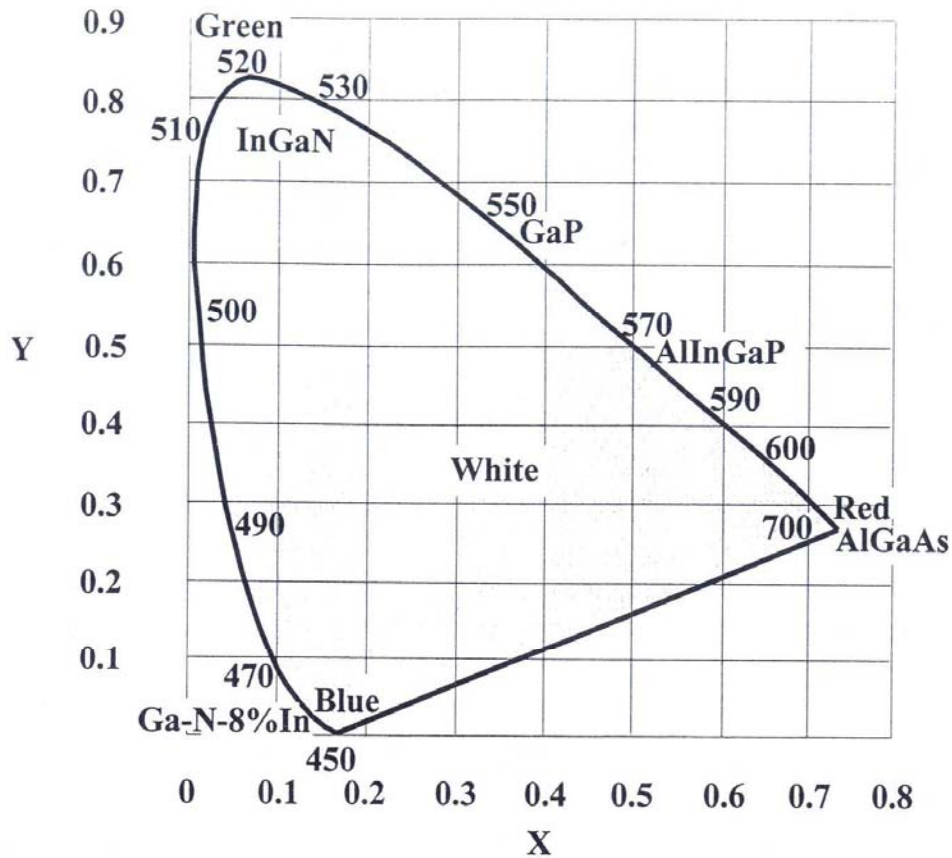
13.8.13 Light-Emitting Diodes (LEDs)

Figure 13.46. Chromaticity diagram in which the positions of some commercially available LEDs are shown.

13.8.14 Liquid Crystal Displays (LCDs)

-LCD s contain peculiar viscous liquids whose rod-shaped molecules are arranged in a specifically ordered pattern : Each of these rod-shaped molecules has a strong electric dipole moment and can be oriented in a glass container and is initially treated so that the molecules on one end are aligned at right angles to the ones on the other end (Fig13.47a)

- If a small voltage is applied to the conducting end faces of the liquid crystal, the molecules align parallel to the field direction and the light is therefore not caused to change its polarization (fig 13.47b)
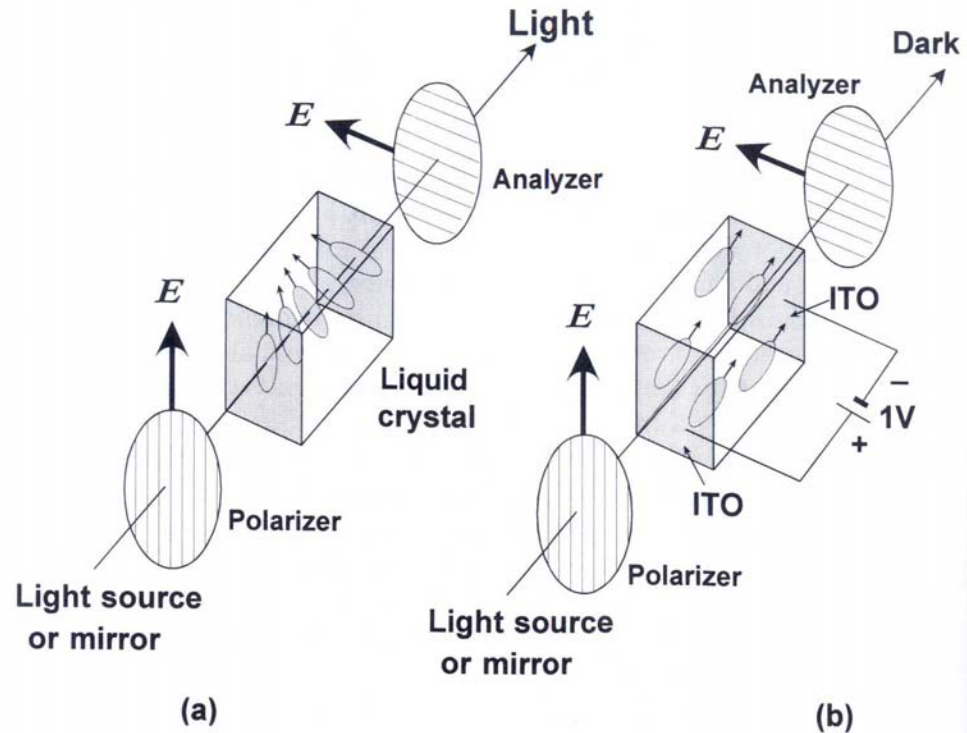

Figure 13.47. Schematic representation of a liquid crystal display unit (a) in the light-transmitting mode, (b) in the non-light-transmitting mode, caused by a potential that is applied to the end faces of the (twisted nematic) liquid crystal. Polarizer and analyzer are identical devices that allow the light (i.e., the electric field vector) to oscillate in only one direction as indicated by arrows (see also Section 13.1.2). The end faces of the liquid crystal–containing glass vessel are coated by transparent electrodes such as indium-tin-oxide (ITO), see Section 9.3.

13.9 Integrated Optoelectronics

13.9.1 Passive Waveguides

- **waveguide** : The interconnecting medium between various optical devices

- It generally consists of a thin, transparent layer whose index of refraction, n_2 is larger than the refractive indices of the two surrounding media, n_1 and n_3

- by undergoing total reflection, the light wave is considered to remain in the center region

- the spatial distribution of the optical energy within all three media is called a mode

- If two boundaries need to be considered, as in the present case, and if the thickness, t of the center region is comparable to the wavelength of light, then the solution of the wave equation yields an electric field distribution

13.9.1 Passive Waveguides

Now, we know from previous calculation (Sec. 4) that under certain conditions additional solutions, i.e., distribution function, do exist (similarly, as a vibrating string can oscillate at higher harmonics)
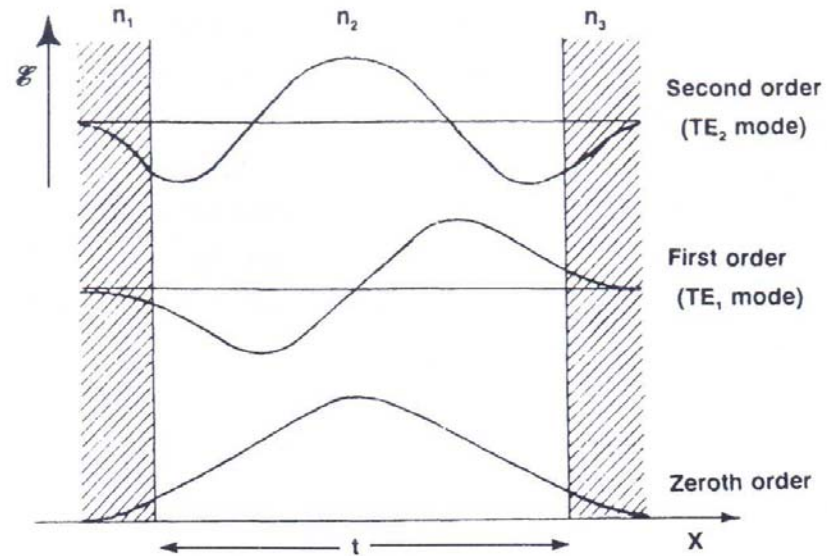

Figure 13.49. Electric field strength distribution (modes) in a waveguide assuming $n_1 = n_3$ (symmetric behavior). The zeroth order and higher-order modes are shown. (Compare with Fig. 4.8.)

In the present case they are called first-order, second-order, etc., modes

13.9 Integrated Optoelectronics

13.9.2 Electro-Optical Waveguides (EOW)

- Fig 13.50

 Schottky-barrier contact which, when reverse biased, forms a wide depletion layer
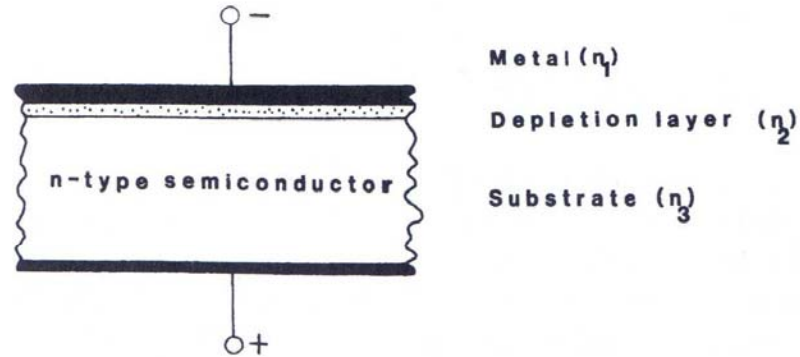

Figure 13.50. Electro-optical waveguide making use of a reverse-biased Schottky-barrier contact. (See also Fig. 8.15.) The light travels in Medium 2 (the depletion layer) when a high-enough voltage is applied to the device.

$$n_2 - n_3 = \frac{e^2 \lambda^2}{2n_3 4\pi^2 \varepsilon_0 m^* c^2}(N_{f3} - N_{f2})$$

For the device to become optical waveguide, the doping of the substrate needs to be reasonably high in order that an appreciable change in the index of refraction is achieved

-The most common application, the compact disk (CD), is a *random-access, read-only* memory device

- The information is stored below a transparent, polymeric medium in the form of bumps, as shown in Fig 13.55

-The CD is read from the back side, i.e., the information is now contained in the form of bumps.

- The aligning of the laser beam on the extremely narrow tracks : three light beam, obtained by dividing into three parts the impinging laser beam shown in Fig. 13.55b utilizing a grating or holographic element
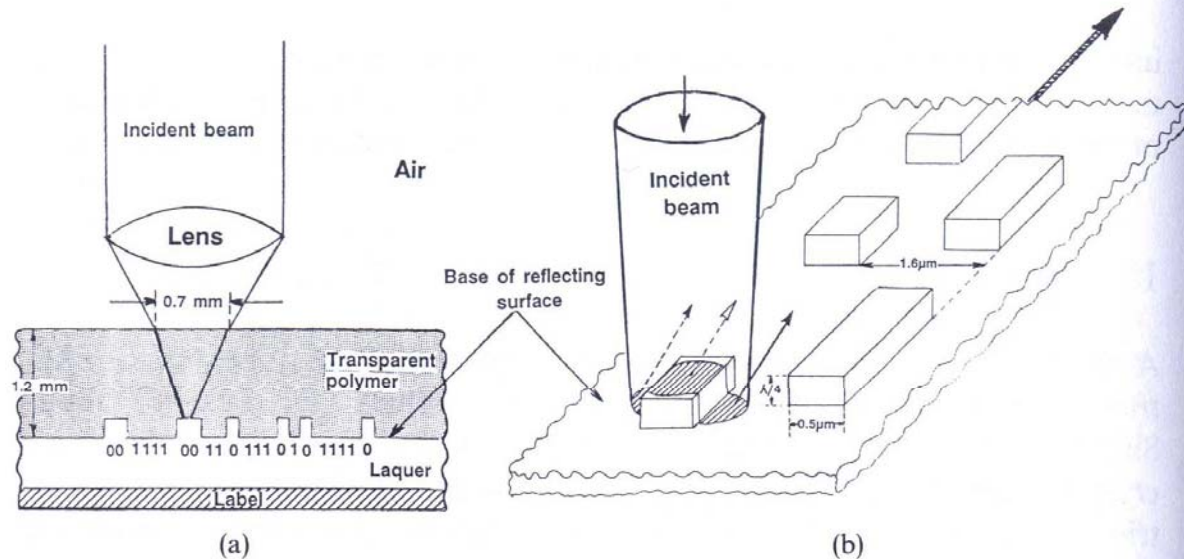

Figure 13.55. Schematic of a compact disk optical storage device. Readout mode. (Not drawn to scale.) The reflected beams in Fig. 13.55(b) are drawn under an angle for clarity. The land and bump areas covered by the probing light have to be of equal size in order that destructive interference can occur (see the hatched areas covered by the incident beam in Fig. 13.55(b)).

Optical transistor : transphasor

-The main element of a transphasor is a small piece of nonlinear optical material which has, similar to a laser, two exactly parallel surfaces at its longitudinal ends

- If the length between the two windows just happen to be an integer multiple of half a wavelength of the light, then constructive interference occurs and the amplitude of the light in the cavity increase rapidly (Fig 13.56a)
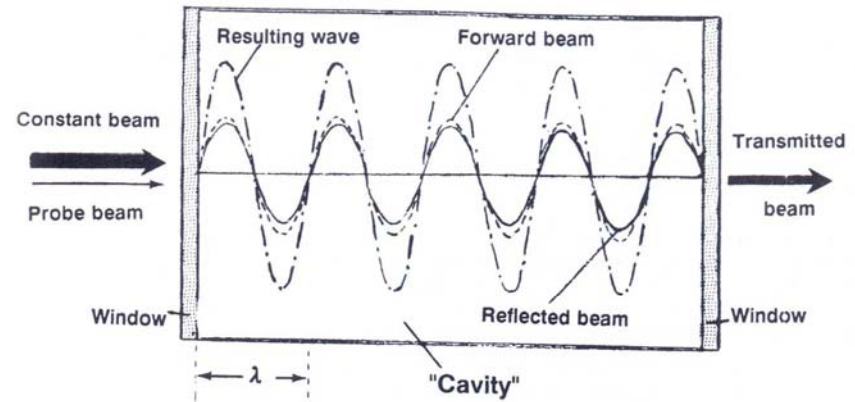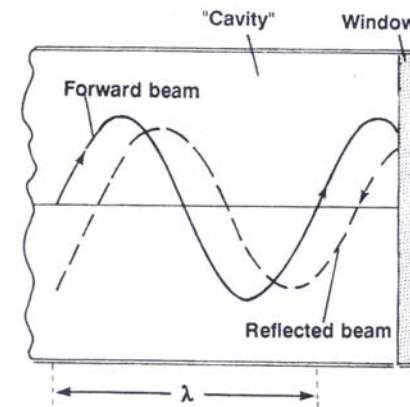
Figure 13.56. Schematic representation of some light waves in a *transphasor*. The reflectivity of the windows is about 90%. (a) Constructive interference. The length of the "cavity" equals an integer multiple of $\lambda/2$. (b) Condition (a) above is not fulfilled. The sum of many forward and reflected beams decreases the total intensity of the light. (*Note*: No phase shift occurs on the boundaries inside the "cavity", because $n_{cavity} > n_{air}$.)

- The key ingredient of a transphasor is a specific substance which changes its index of refraction as a function of the intensity of light, the index of refraction is

$$n_{med} = \frac{c_{vac}}{c_{med}} = \frac{\lambda_{vac}}{\lambda_{med}}$$

- Optical switch in involves a "constant laser beam" whose intensity is not yet strong enough to trigger constructive interference (Fig 13.56a). This light intensity is supplemented by a second laser beam, the "probe beam," which is directed onto the same spot of the window of the transphasor and which provides the extra light energy to trigger a large change in n and thus constructive interference (Fig,13.57)
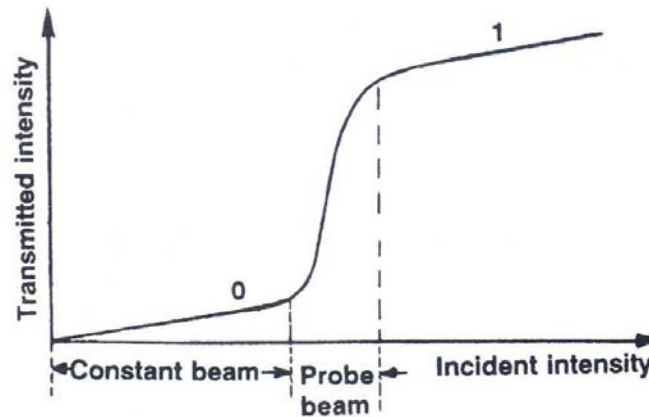
Figure 13.57. Schematic representation of an optical AND gate as obtained from an optical transistor (transphasor) constructed from a material with nonlinear refractive index. The low transmission state may represent a "zero" in binary logic, whereas the high transmission of light may stand for a "one."

(continued) All taken, a small intensity change caused by the probe beam invokes a large intensity of the transmitted beam. This combination of two signals that interact with a switching device can be utilized as an "AND" logic circuit (See Sec. 8.7.12). Likewise "OR" gates (either of the two beams is already strong enough to trigger critically a change in n) or "NOT" gate (which involve the reflected light) can be constructed

X-rays : Electromagnetic radiation of energy higher than that characteristic for UV light

- For its production, a beam of electrons emitted from a hot filament is accelerated in high electric field toward a metallic electrode. On impact, the energy of the electrons is lost either by **white X-radiation**, that is, in the form of continuous spectrum (within limits), or by essentially monochromatic X-ray (called **characteristic X-ray**) that are specific for the target material

-The white X-ray are emitted as a consequence of the deceleration of the electrons in the electric field of a series of atoms.

The maximum energy that can be emitted this way

$$E_{max} = eV = h\nu = \frac{hc}{\lambda} \qquad , \qquad \lambda = \frac{12.4}{V}$$

13.12 X-Ray Emission

- The voltage dependence of several white X-ray spectra (Fig 13.58)

- The wavelength of characteristic X-rays depends on the material on which the accelerated electrons impinge :

- K_α X-Ray (Fig 13.59)

  For Cu :1.542Å

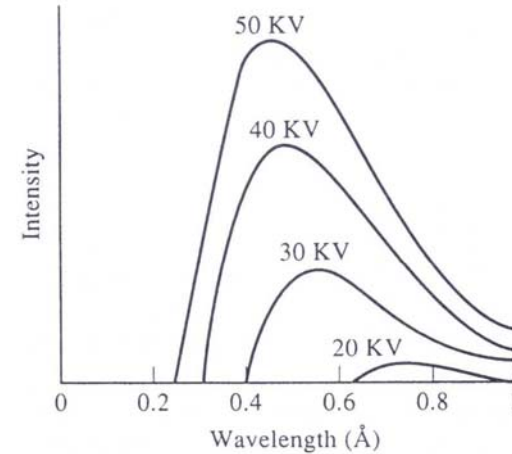- X-ray is used in material science for investigating the crystal structure of materials

Figure 13.58. Schematic representation of the wavelength dependence of the intensity of white X-ray emission for selected acceleration voltages.
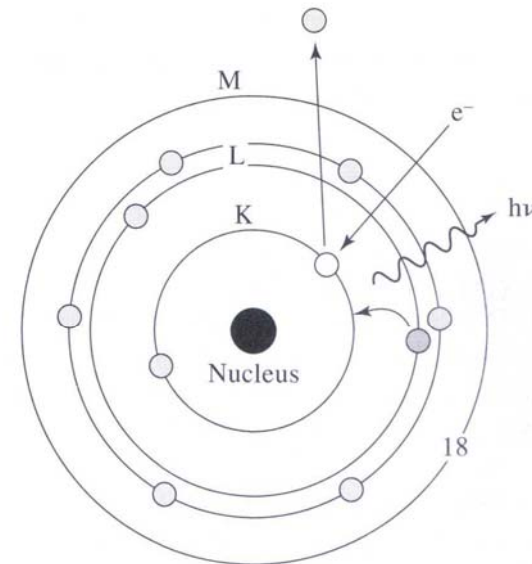

Figure 13.59. Schematic representation of the emission of characteristic X-radiation by exciting a K-electron and refilling the vacancy thus created with an L-electron.